

Molecular Physics

An International Journal at the Interface Between Chemistry and Physics

ISSN: (Print) (Online) Journal homepage: www.tandfonline.com/journals/tmph20

Two state model for the ML-BOP potential

Numa Zorzi, Andreas Neophytou & Francesco Sciortino

To cite this article: Numa Zorzi, Andreas Neophytou & Francesco Sciortino (26 Sep 2024): Two state model for the ML-BOP potential, Molecular Physics, DOI: [10.1080/00268976.2024.2407025](https://doi.org/10.1080/00268976.2024.2407025)

To link to this article: <https://doi.org/10.1080/00268976.2024.2407025>



Published online: 26 Sep 2024.



Submit your article to this journal [↗](#)



View related articles [↗](#)



View Crossmark data [↗](#)

Two state model for the ML-BOP potential

Numa Zorzi , Andreas Neophytou and Francesco Sciortino 

Department of Physics, Sapienza University of Rome, Roma, Italy

ABSTRACT

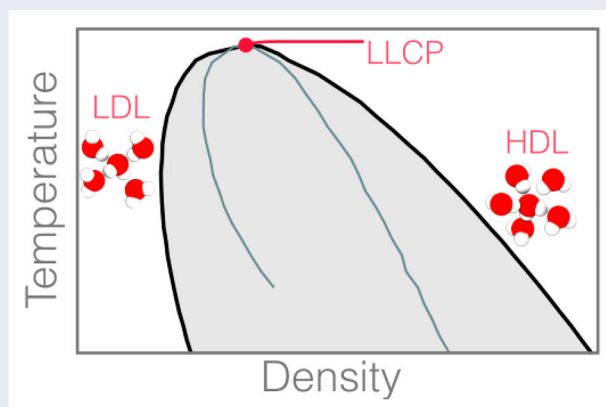
The coarse-grained machine-learning derived ML-BOP model [Chan et al., *Nature Commun.* **10**, 379 (2019)] provides a monoatomic representation of the water-water interaction potential in which orientational interactions are included as three-body contributions. Despite its simplicity, the model reproduces the phase diagram of water and its anomalies. Here, we show that a two-state Gibbs free energy expression – fitted simultaneously on the temperature and pressure dependence of the density and internal energy – predicts the existence of a liquid–liquid critical point, with critical parameters consistent with previous estimates. We also show that in this model: (i) while the low density liquid is pre-empted by crystal nucleation, the high-density liquid and its spinodal are accessible in numerical studies down to 100 K; (ii) crystallisation requires the presence of a local low density region. Thus, for densities larger than the critical density, spinodal decomposition (or nucleation of the low-density liquid) is a pre-requisite for ice nucleation.

ARTICLE HISTORY

Received 28 June 2024
Accepted 4 September 2024

KEYWORDS

Liquid–liquid critical point; two state model; machine learning; supercooled water; spinodal decomposition



1. Introduction

Modelling water *in silico* has a long history, dating back to the origin of numerical simulation [1–6]. The relevance of water in the life of biological organisms, in material science, in atmospheric predictions as well as in planetary science has driven the scientific community to develop better and better models that are able to describe water across different phases. Recently, the *ab-initio* MB-pol model [7, 8] has been shown able to reproduce (with a precision of approximately 10 K) the coexistence between the liquid and crystal phases of water, as well as its crystal-crystal lines [9]. At the same time, efforts in the last decade have been pushed in the direction of finding simpler coarse-grained descriptions for the interactions between water molecules which can (over a limited range

of pressure and temperature) still provide a reasonably accurate modelling of water's thermodynamics [10–13].

In the last years, machine learning approaches have started to contribute to this methodology by optimising the parameters of a pre-selected functional form. In the case of the machine-learned bond-orientational parameter model (ML-BOP) [14], each water molecule is represented by a single interacting site and the potential includes a combination of two- and three-body interactions based off the Tersoff potential (in the same spirit as the mW model [12, 15]). The resulting short-ranged potential is computationally efficient and able to provide an accurate modelling of the liquid-ice coexistence curve and of the isobaric temperature dependence of the density [14].

Some properties of this model have been studied in a recent series of articles [16–20]. In deep supercooled states volume (V) and enthalpy (H) fluctuations grow significantly, indicating the presence of a liquid–liquid critical point (LLCP) located just below the homogeneous nucleation line of the model [19, 20]. Extrapolations based on the potential energy landscape approach [20, 21] and analysis of very short-time (up to a few hundred nanoseconds) density fluctuations in the time window prior to crystal nucleation [19] consistently predict the existence of a LLCP for the model at a critical temperature of $T_c \approx 181$ K and a critical pressure P_c between 170 MPa [19] and 175 MPa [20].

The location of the LLCP inside the region of the phase diagram where homogeneous nucleation occurs could, at first sight, suggest that it is irrelevant for understanding the properties of the supercooled liquid phase. In reality the LLCP, as with any other second-order critical point, is the origin of several lines of extrema (such as the compressibility and the specific heat), commonly grouped together within the Widom line framework [22]. These lines of extrema originate in the supercooled region, however they extend to regions of the phase diagram where liquid water is the stable phase. In different terms, the critical point induces a modulation of the free energy surface whose effects can be detected well above T_c . In the past, several functional forms for the free-energy (grouped under the umbrella of two-state models) have been proposed for water, starting from early work limited to low temperatures [23, 24] and progressively improved to model wider and wider regions of pressure and temperature [25–32]. The functional forms have been compared and parameterised against data for several molecular models of water [25–30, 32] and to real water as well [31], in order to provide support for the compatibility of such a thermodynamic model with a LLCP, as well as to detect the location of the critical point.

In this article we aim to investigate the relevance of a metastable LLCP to the thermodynamics and phase behaviour of supercooled water (as modelled by the ML-BOP potential). First, we apply a two-state model to the ML-BOP system with the aim of identifying whether it can provide support to the critical point estimates provided in Refs. [19, 20]. We show that indeed a two-state model incorporating the physics of the LLCP properly describes the ML-BOP free-energy surface. The predicted expression is not only able to reproduce the density and energy in the pressure and temperature window where ML-BOP data are available, but also the compressibility and the specific heat (quantities related to the curvature of the free energy). Second, we investigate the low temperature region where crystallisation does not

take place in μ s long simulations with the aim of calculating the high-density liquid (HDL) spinodal and to prove that crystal nucleation events take place only in the vicinity of such a line. This has two important consequences: (i) it proves that even if the LLCP is dominated by crystal nucleation, the physics of the critical point is accessible to investigation in the region where the HDL is favoured over the low-density liquid (LDL) phase; (ii) it shows that nucleation takes place only inside and close to the HDL spinodal, strongly suggesting that crystallisation is slaved to the nucleation process of the LDL.

2. Computational details

We have numerically studied a system of $N = 2000$ water molecules interacting via the ML-BOP potential by performing a series of molecular dynamics simulations in the NVT and NPT ensembles using LAMMPS (version 2Aug2023) [34]. Simulations were performed for a large range of state points which cover densities between $\rho = 0.9$ g/cm³ and $\rho = 1.35$ g/cm³, temperatures between $T = 100$ K and $T = 270$ K and pressures between $P = 1$ bar and $P = 7000$ bar. The integration time step was progressively increased from 1 fs at $T = 270$ K to 5 fs at $T = 100$ K. Note that ML-BOP, being a coarse-grained model, has dynamics that are much faster than real water. In addition, being a short-range potential and monoatomic, ML-BOP systems can be simulated for time scales much longer than is possible with molecular models which include explicit charges (commonly up to few μ s at the lowest T). The investigated state points for the NVT simulations are indicated as symbols in Figure 1.

3. Results

3.1. Two-state fit

In a two-state mixture model, molecules are assumed to belong to two distinct classes, with two different local environments. Each of the two states includes a continuum of local geometries. Only recently have sophisticated order parameters been developed to highlight this bimodal distribution of local environments in supercooled water [26, 35–38]. For convenience we will refer to molecules belonging to one of these two broad families of local environments as either low- (LDM) or high-density (HDM) molecules, in analogy with the LDL and HDL phases which appear below the LLCP.

We assume, that the system Gibbs free energy *per particle* can be written as [28, 31, 39]

$$g(P, T) = g_{\text{HDM}}(P, T) + \psi \Delta g(P, T) + k_{\text{B}}T [\psi \ln \psi + (1 - \psi) \ln(1 - \psi)]$$

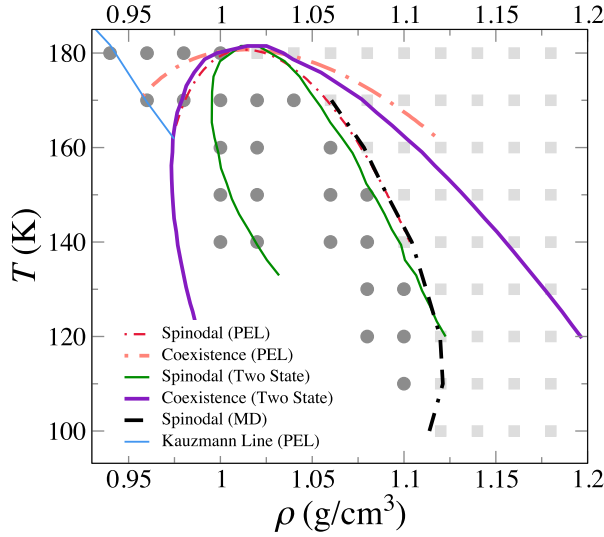


Figure 1. Graphical representation of the spinodal and coexistence lines of the ML-BOP potential. Lines marked (PEL) are reproduced from Ref. [20]. The faint squares represent state points where the system is metastable in the liquid phase on the 100 ns scale, while the filled circles represent state points where crystallisation is observed. The Kauzmann [33] line is defined as the locus where the configurational entropy of the liquid vanishes [20].

$$+ J\psi(1 - \psi), \quad (1)$$

where g_{HDM} represents the Gibbs free energy per particle for a liquid of HDMs, ψ is the fraction of LDMs, Δg is the difference in Gibbs free energy per particle between the two structures and J is a coefficient measuring the strength of the non-ideality of mixing. We assume J to have no temperature dependence. This means that mixing is solely due to the non-ideal contribution of the energy [40]. In practice, this means we express J as $J(P) = k_{\text{B}}T_c(2 + \omega_0(P/P_c - 1))$, where ω_0 is a fitting parameter given in Table A1. This is the same analytic form as in [31], where a two-state model is used to describe the experimental behaviour of water. This form ensures that at the critical point we respect the condition $J(P_c) = 2k_{\text{B}}T_c$ [40]. The contribution $\psi \ln \psi + (1 - \psi) \ln(1 - \psi)$ is the standard mixing entropy term, and we choose to model g_{HDM} as

$$g_{\text{HDM}}(T, P) = g^A(\tilde{P}) + g^B(\tilde{P})\tilde{T} + g^C(\tilde{P})\tilde{T} \log \tilde{T}, \quad (2)$$

where $\tilde{P} = P/P_c$ and $\tilde{T} = T/T_c$. We make this choice since it ensures the correct T dependence of the ideal-gas contribution (a similar functional form for the free energy per particle has previously been proposed [41]). The functions $g^A(\tilde{P})$, $g^B(\tilde{P})$ and $g^C(\tilde{P})$ are assumed to be polynomial (up to the second order) in \tilde{P} . Expressions for these functions are provided in Appendix 2.

Since LDMs and HDMs are in chemical equilibrium, their chemical potentials must be identical, which leads

to the following equation [39],

$$\Delta g + k_{\text{B}}T \ln \frac{\psi}{1 - \psi} + J(1 - 2\psi) = 0, \quad (3)$$

which can be numerically solved to determine ψ for a given state point. Finally, we express Δg as a third order polynomial in $\hat{T} = T/T_c - 1$ and $\hat{P} = P/P_c - 1$,

$$\Delta g = \sum_{i=0}^3 \sum_{j=0}^{3-i} a_{ij} \hat{T}^i \hat{P}^j \quad (4)$$

Note that since at the critical point $g_{\text{HDM}} = g_{\text{LDM}}$ (and hence $\Delta g(T_c, P_c) = 0$), the coefficient a_{00} is fixed to the value $a_{00} = 0$. In total, the free energy expression requires 19 parameters. T_c and P_c are not included in the fit and constrained to the values proposed in Ref. [20]. We fit simultaneously over density and energy, by optimising the following merit function:

$$\sigma^2 \equiv \frac{(V - V_0)^2}{\bar{V}^2} + \frac{(E - E_0)^2}{\bar{E}^2}$$

where V_0, E_0 are the target quantities and \bar{V}, \bar{E} are the averages of the entire dataset. The best-fit parameters are reported in Table A1.

Figure 2(a,b) show the P and T dependence for the density and internal energy, respectively, for the two-state model of the ML-BOP system compared to those determined numerically. Note that at low pressure crystallisation prevents the possibility to add further low temperature state points. The associated T and P dependence for the fraction of LDMs (ψ) is presented in Figure 3, which shows that below P_c the fraction of LDMs continuously increases as temperature decreases, whereas above P_c it discontinuously jumps (as indicated by the dashed lines) from a value $\psi < 0.5$ to one where $\psi > 0.5$. Additionally, at $P = P_c$ and $T = T_c$ the model gives $\psi = 0.5$, as would be expected. This confirms that the two-state model used here reproduces the critical behaviour of the ML-BOP model from Refs. [19, 20].

A further test for the quality of the fit is reported in Figure 4, where the predicted isothermal compressibility κ_T and constant pressure specific heat c_p are compared with the appropriate derivatives of the Gibbs free energy. κ_T and c_p are directly evaluated from the simulations via the fluctuation formulas

$$\kappa_T = \frac{\langle \Delta V^2 \rangle}{Nk_{\text{B}}T\langle V \rangle}, \quad c_p = \frac{\langle \Delta H^2 \rangle}{Nk_{\text{B}}T^2} \quad (5)$$

where $\langle \Delta V^2 \rangle$ and $\langle \Delta H^2 \rangle$ indicate the squared variance of the volume and enthalpy fluctuations, respectively, and $\langle V \rangle$ the average volume. As Figure 4 shows, these quantities – which correspond to second derivatives of the Gibbs free energy – are also properly reproduced by the two state model, except at the boundary of the data set.

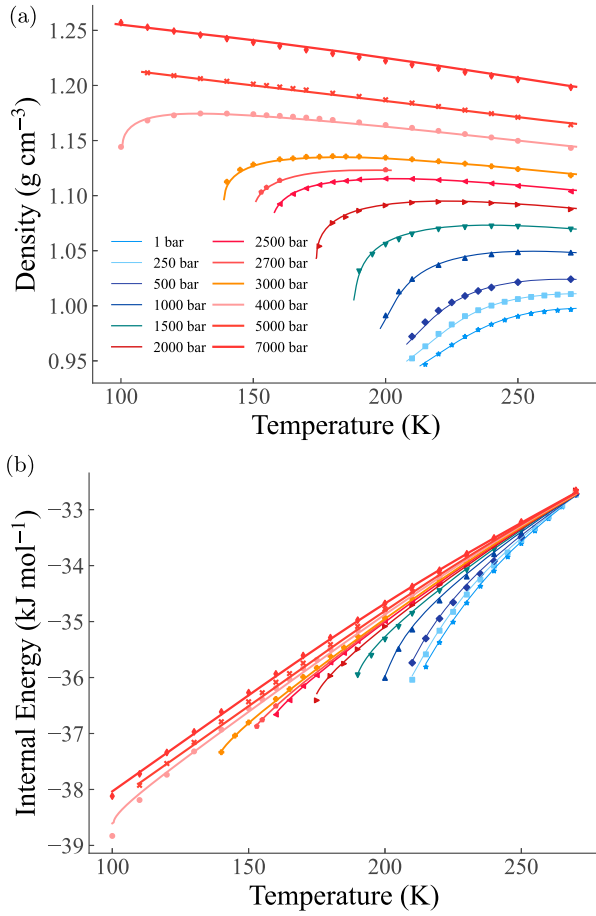


Figure 2. (a) Density as a function of temperature along selected isobars. The lines are obtained using the two-state model and the points represent simulation data. Uncertainties are smaller than the points. (b) Internal energy $U(P, T)$ as a function of temperature along selected isobars.

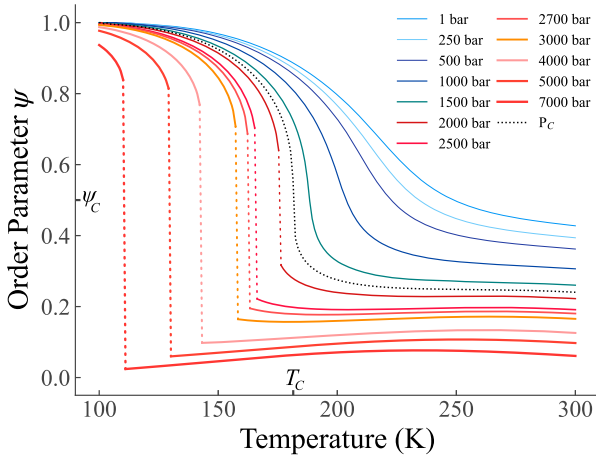


Figure 3. Order parameter (ψ) as a function of temperature along selected isobars. The value of ψ is obtained by numerically solving Equation (3).

3.2. HDL spinodal and ice nucleation

The fast dynamics and computational efficiency afforded by the ML-BOP model makes it possible to equilibrate

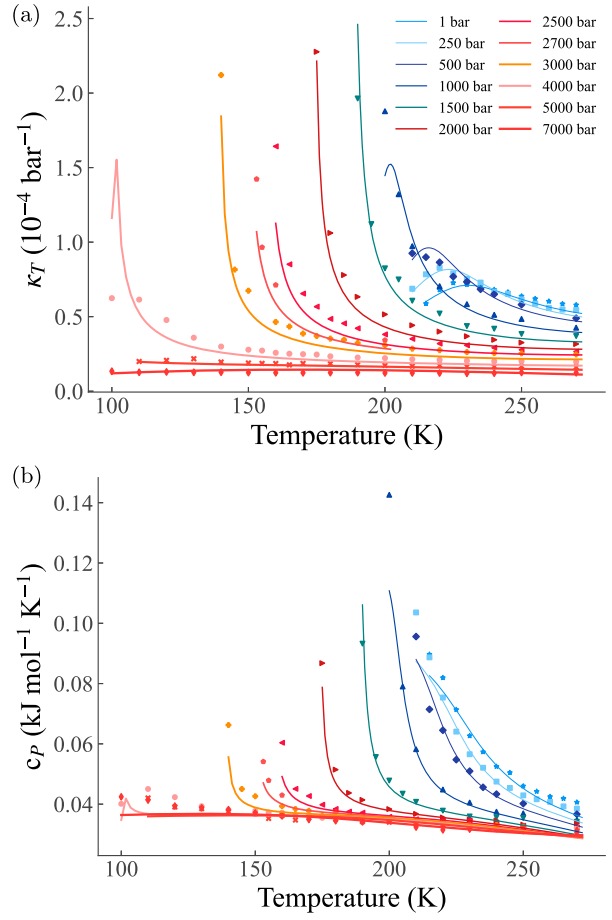


Figure 4. (a) Isothermal compressibility (κ_T) as a function of temperature along selected isobars. (b) Constant pressure molar heat (c_p) as a function of temperature along selected isobars.

systems, with a reasonable effort, even at low temperatures (~ 100 K). In the low density region, crystallisation (see black squares in Figure 1) prohibits the calculation of equilibrium data for the liquid (the lifetime of the LDL is on the ns scale due to the similarity of the local tetrahedral coordination of the liquid and crystalline structures). However, in the high density region no crystallisation events are observed on the time scales considered. This makes it possible to numerically evaluate the equation of state (EOS) of the HDL. The resulting isotherms are shown in Figure 5, together with the corresponding isotherms predicted by the two-state model. The isotherms show a clear trend to flatten out at low density, indicating the approach of a spinodal instability. Note that, while it is impossible to calculate the coexistence line since the coexisting LDL cannot be equilibrated, the high density spinodal is properly defined and, in principle, amenable to experimental verification.

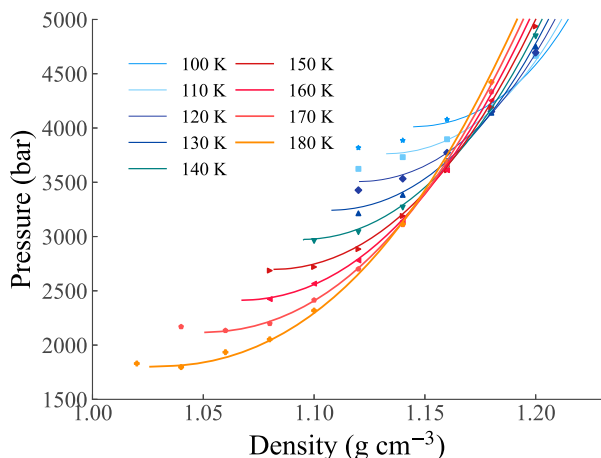


Figure 5. Different isotherms for the high-density liquid (HDL) phase where points are determined numerically from NVT molecular dynamics simulations and lines from the equation-of-state (EOS) computed from the two-state model.

A quadratic fit of the numerically determined HDL EOSs (limited to $P < 5$ kbar) using the mean-field relation,

$$P(V) = P_{\text{spinodal}} + A(V - V_{\text{spinodal}})^2, \quad (6)$$

provides the coordinates of the HDL spinodal for a given temperature [42], which is plotted in Figure 1.

The two-state Gibbs free energy allows us to evaluate the coexistence pressure in the region of temperatures where more than one solution for ψ exists. To do so we search along an isotherm for the two values of ψ with identical Gibbs free energy and pressure. To calculate instead the spinodal curves, we evaluate $V(P)$ for both phases searching, again along an isotherm, for the two values of ψ for which $\frac{\partial P}{\partial V}|_T = 0$. The results are shown in Figure 1 together with the corresponding lines obtained in [20]. The HD spinodal tracks well the numerical estimates for the spinodal Equation (6). On the LD side, only the PEL estimate of the spinodal is available [20] and the difference with the two-state spinodal is larger. We attribute this discrepancy to the absence of equilibrium data on the low density side, due to the fast crystallisation. A similar pattern is seen also in the coexistence lines. We observe a certain degree of discrepancy between the PEL line and the two-state coexistence line. This is again due to the absence of LD data in the two-state model, an issue that is now relevant also for the HD side of the coexistence line. Indeed, coexistence curves require simultaneous information about both the LD and HD phases. We also want to stress that at lower temperatures the lines are subject to greater uncertainty, due to the decreasing amount of data available for lower temperatures.

Interestingly, we note that a re-entrant behaviour upon cooling both for the coexistence and spinodal line, in agreement with the finding of [19]. Moreover, it is quite interesting to observe that the spinodal line approximately marks the separation between the crystallizing (circles in Figure 1) and the non-crystallizing state points (squares in Figure 1). This indicates that crystallisation takes place only in the LDL. Only when a nucleus of the LDL appears (either via nucleation outside the spinodal region or by spinodal decomposition) can the crystallisation process begin. The fast nucleation of the nascent LDL is consistent with the experimental observation of the liquid–liquid transition in bulk supercooled water under pressure [43].

4. Conclusions

In this article we have shown that the Gibbs free energy of the ML-BOP model (a machine-learned coarse-grained model for water) is properly described by a thermodynamic model which assumes that the molecules can adopt one of two distinct local environments – a low-density and high-density environment – and the interaction between the two environments is strong enough to induce a liquid–liquid critical point (LLCP). The LLCP of the ML-BOP model is located just below the homogeneous nucleation and thus it cannot be directly observed due to the onset of crystallisation, although, signatures of the LLCP have been observed in simulations for systems with less than 200 molecules [19]. This is distinct from previously studied models of water displaying a LLCP [32, 44–47], and so, the ML-BOP model offers the possibility to answer the question of whether the existence of a LLCP is of any significance when it cannot be directly accessed. This question is of importance since experiments also suggest that close to the LLCP crystallisation takes place on the sub- μs scale [43], a time interval that barely allows for the equilibration of the low-density liquid (LDL) before solidification takes over.

This article offers some elements to formulate such an answer. First of all, the two-state model fit shows that the shape of the free-energy surface is strongly influenced by the presence of the LLCP. Additionally, the presence of a LLCP explains the thermodynamic behaviour of the liquid close to its metastable region: the compressibility and specific heat anomalies are linked to its existence. Second, and more importantly, while the LLCP is technically not accessible, the spinodal of the high-density liquid (HDL) can be clearly detected and appears to emanate from the non-accessible critical point. The HDL is found to exist over a wide range of densities and temperatures. Only when the HDL is brought (by a change in the pressure or

in the temperature) close to, or below, its spinodal does the very rapid formation of the crystal take place. The coincidence of the homogeneous nucleation line with the HDL spinodal is very strong evidence for the importance of the physics of the LLCP, even if the LLCP itself can not be accessed.

Disclosure statement

No potential conflict of interest was reported by the author(s).

Funding

We dedicate this manuscript to Professors Abascal and Rull for their important contribution to the physics of liquids, including water. We acknowledge support from MIUR-PRIN 2022JWAF7Y, Cineca ISCRAB initiative and ICSC-Centro Nazionale di Ricerca in High Performance Computing, Big Data and Quantum Computing, funded by the European Union 'NextGenerationEU'.

Data Availability Statement

The data that support the findings of this study are available within the article. The public domain LAMMPS code has been used to generate the trajectories for all different state points.

ORCID

Numa Zorzi  <https://orcid.org/0009-0006-3619-3790>

Francesco Sciortino  <http://orcid.org/0000-0002-2418-2713>

References

- [1] J. Barker and R. Watts, *Chem. Phys. Lett.* **3**, 144 (1969). doi:10.1016/0009-2614(69)80119-3
- [2] A. Rahman and F.H. Stillinger, *J. Chem. Phys.* **55**, 3336 (1971). doi:10.1063/1.1676585
- [3] F.H. Stillinger and A. Rahman, *J. Chem. Phys.* **57**, 1281 (1972). doi:10.1063/1.1678388
- [4] A. Ben-Naim and F. Stillinger, *8 Aspects of the Statistical-Mechanical Theory of Water*, edited by R. Horne (Water and Aqueous Solutions, Wiley, New York, 1972).
- [5] O. Matsuoka, E. Clementi, and M. Yoshimine, *J. Chem. Phys.* **64**, 1351 (1976). doi:10.1063/1.432402
- [6] W. Bol, *Mol. Phys.* **45**, 605 (1982). doi:10.1080/00268978.200100461
- [7] S.K. Reddy, S.C. Straight, P. Bajaj, C. Huy Pham, M. Riera, D.R. Moberg, M.A. Morales, C. Knight, A.W. Götz, and F. Paesani, *J. Chem. Phys.* **145**, 194504 (2016). doi:10.1063/1.4967719
- [8] X. Zhu, M. Riera, E.F. Bull-Vulpe, and F. Paesani, *J. Chem. Theory Comput.* **19**, 3551 (2023). doi:10.1021/acs.jctc.3c00326
- [9] S.L. Bore and F. Paesani, *Nat. Comm.* **14**, 3349 (2023). doi:10.1038/s41467-023-38855-1
- [10] J.L. Abascal and C. Vega, *J. Chem. Phys.* **123**, 234505 (2005). doi:10.1063/1.2121687
- [11] J. Abascal, E. Sanz, R. García Fernández, and C. Vega, *J. Chem. Phys.* **122**, 234511 (2005). doi:10.1063/1.1931662
- [12] V. Molinero and E.B. Moore, *J. Phys. Chem. B* **113**, 4008 (2009). doi:10.1021/jp805227c
- [13] G. Franzese, L. Coronas, and O. Vilanova, A transferable molecular model for accurate thermodynamic studies of water in large-scale systems, 16 April 2024, PREPRINT (Version 1) available at Research Square [<https://doi.org/10.21203/rs.3.rs-4243098/v1>]
- [14] H. Chan, M.J. Cherukara, B. Narayanan, T.D. Loeffler, C. Benmore, S.K. Gray, and S.K. Sankaranarayanan, *Nat. Comm.* **10**, 379 (2019). doi:10.1038/s41467-018-08222-6
- [15] E.B. Moore and V. Molinero, *Nature* **479**, 506 (2011). doi:10.1038/nature10586
- [16] D. Dhabal, S.K. Sankaranarayanan, and V. Molinero, *J. Phys. Chem. B* **126**, 9881 (2022). doi:10.1021/acs.jpcc.2c06246
- [17] D. Dhabal and V. Molinero, *J. Phys. Chem. B* **127**, 2847 (2023). doi:10.1021/acs.jpcc.3c00434
- [18] P.A. Taylor and M.J. Stevens, *Eur. Phys. J. E* **46**, 97 (2023). doi:10.1140/epje/s10189-023-00355-x
- [19] D. Dhabal, R. Kumar, and V. Molinero, *Proc. Natl. Acad. Sci. U. S. A.* **121**, e2322853121 (2024). doi:10.1073/pnas.2322853121
- [20] A. Neophytou and F. Sciortino, *J. Chem. Phys.* **160**, 114502 (2024). doi:10.1063/5.0197613
- [21] F.H. Stillinger, *Energy Landscapes, Inherent Structures, and Condensed-Matter Phenomena* (Princeton University Press, 2015).
- [22] L. Xu, P. Kumar, S.V. Buldyrev, S.-H. Chen, P.H. Poole, F. Sciortino, and H.E. Stanley, *Proc. Natl. Acad. Sci. U. S. A.* **102**, 16558 (2005). doi:10.1073/pnas.0507870102
- [23] C.T. Moynihan, *MRS Online Proc. Libr.* **455**, 411 (1996). doi:10.1557/PROC-455-411
- [24] E. Ponyatovsky, V. Sinitsyn, and T. Pozdnyakova, *J. Chem. Phys.* **109**, 2413 (1998). doi:10.1063/1.476809
- [25] M.J. Cuthbertson and P.H. Poole, *Phys. Rev. Lett.* **106**, 115706 (2011). doi:10.1103/PhysRevLett.106.115706
- [26] J. Russo and H. Tanaka, *Nat. Comm.* **5**, 3556 (2014). doi:10.1038/ncomms4556
- [27] V. Holten, J.C. Palmer, P.H. Poole, P.G. Debenedetti, and M.A. Anisimov, *J. Chem. Phys.* **140**, 104502 (2014). doi:10.1063/1.4867287
- [28] R.S. Singh, J.W. Biddle, P.G. Debenedetti, and M.A. Anisimov, *J. Chem. Phys.* **144**, 144504 (2016). doi:10.1063/1.4944986
- [29] J.W. Biddle, R.S. Singh, E.M. Sparano, F. Ricci, M.A. González, C. Valeriani, J.L. Abascal, P.G. Debenedetti, M.A. Anisimov, and F. Caupin, *J. Chem. Phys.* **146**, 034502 (2017). doi:10.1063/1.4973546
- [30] H. Tanaka, *J. Chem. Phys.* **112**, 799 (2000). doi:10.1063/1.480609
- [31] F. Caupin and M.A. Anisimov, *J. Chem. Phys.* **151**, 034503 (2019). doi:10.1063/1.5100228
- [32] J. Weis, F. Sciortino, A.Z. Panagiotopoulos, and P.G. Debenedetti, *J. Chem. Phys.* **157**, 024502 (2022). doi:10.1063/5.0099520
- [33] W. Kauzmann, *Chem. Rev.* **43**, 219 (1948). doi:10.1021/cr60135a002

- [34] A.P. Thompson, H.M. Aktulga, R. Berger, D.S. Bolinteanu, W.M. Brown, P.S. Crozier, P.J. in't Veld, A. Kohlmeyer, S.G. Moore, T.D. Nguyen, R. Shan, M.J. Stevens, J. Tranchida, C. Trott, and S.J. Plimpton, *Comput. Phys. Commun.* **271**, 108171 (2022). doi:10.1016/j.cpc.2021.108171
- [35] R. Foffi and F. Sciortino, *J. Chem. Phys.* **160**, 090901 (2024). doi:10.1063/5.0188764
- [36] R. Foffi and F. Sciortino, *J. Phys. Chem. B* **127**, 378 (2022). doi:10.1021/acs.jpcc.2c07169
- [37] C. Faccio, M. Benzi, L. Zanetti-Polzi, and I. Daidone, *J. Mol. Liq.* **355**, 118922 (2022). doi:10.1016/j.molliq.2022.118922
- [38] A. Neophytou, D. Chakrabarti, and F. Sciortino, *Nat. Phys.* **18**, 1248 (2022). doi:10.1038/s41567-022-01698-6
- [39] V. Holten and M. Anisimov, *Sci. Rep.* **2**, 713 (2012). doi:10.1038/srep00713
- [40] V. Holten, D.T. Limmer, V. Molinero, and M.A. Anisimov, *J. Chem. Phys.* **138**, 174501 (2013). doi:10.1063/1.4802992
- [41] A. Amadei, M. Apol, and H. Berendsen, *J. Chem. Phys.* **109**, 3004 (1998). doi:10.1063/1.476893
- [42] P.H. Poole, F. Sciortino, U. Essmann, and H. Stanley, *Phys. Rev. E* **48**, 3799 (1993). doi:10.1103/PhysRevE.48.3799
- [43] K.H. Kim, K. Amann-Winkel, N. Giovambattista, A. Späh, F. Perakis, H. Pathak, M.L. Parada, C. Yang, D. Mariedahl, T. Eklund, T.J. Lane, S. You, S. Jeong, M. Weston, J.H. Lee, I. Eom, M. Kim, J. Park, S.H. Chun, P.H. Poole, and A. Nilsson, *Science* **370**, 978 (2020). doi:10.1126/science.abb9385
- [44] P.H. Poole, F. Sciortino, U. Essmann, and H. Stanley, *Nature* **360**, 324 (1992). doi:10.1038/360324a0
- [45] P.G. Debenedetti, F. Sciortino, and G.H. Zerze, *Science* **369**, 289 (2020). doi:10.1126/science.abb9796
- [46] F. Sciortino, Y. Zhai, S.L. Bore, and F. Paesani, *chemrxiv.org* (2024).
- [47] L.E. Coronas and G. Franzese, *arXiv preprint arXiv:2405.10181* (2024).

Appendices

Appendix 1. Model parameters

Table A1. Best-fit parameters of the two-state model. ω_0 is dimensionless while all other parameters are in kJ mol^{-1} .

Parameter	Value	Parameter	Value
g_0^A	-4.106e1	a_{10}	2.729
g_1^A	2.291	a_{01}	7.031e-1
g_2^A	2.316e-2	a_{20}	-2.584
g_0^B	2.903e1	a_{11}	-3.721e-1
g_1^B	4.378e-1	a_{02}	-6.663e-2
g_2^B	-4.821e-2	a_{30}	2.239
g_0^C	-5.494	a_{21}	1.285
g_1^C	-4.272e-1	a_{12}	8.969e-2
g_2^C	5.571e-2	a_{03}	-3.008e-3
ω_0	1.174e-4		

Appendix 2. The model for g_{HDM}

The full expression for g_{HDM} is

$$\begin{aligned}
 g_{\text{HDM}} = & g_0^A + g_1^A \tilde{P} + g_2^A \tilde{P}^2 \\
 & + (g_0^B + g_1^B \tilde{P} + g_2^B \tilde{P}^2) \tilde{T} \\
 & + (g_0^C + g_1^C \tilde{P} + g_2^C \tilde{P}^2) \tilde{T} \log \tilde{T}, \quad (\text{A1})
 \end{aligned}$$

where $\tilde{T} = T/T_c$ and $\tilde{P} = P/P_c$. Note that the selected functional forms for the LD and HD phases can result in descriptions of the pure low- and high-density liquids which can have density and compressibility extremes. In our case, the minimisation procedure does indeed generate weak density anomalies, which are amplified if extrapolating at temperatures where no simulation data are available due to crystal formation. In the future, it will be interesting to attempt to model the free energy of the pure phases with functional form analytically constrained to behave regularly.